Am J Transl Res 2021;13(11):12410-12420
www.ajtr.org /ISSN:1943-8141/AJTR0134834

Original Article

Identification of pathways and genes associated with meniscus degeneration using bioinformatics analyses

Hui Huang[1*], Jiaxuan Zheng[2*], Ming Deng[3*], Yehan Fang[1], Daolu Zhan[4], Guangji Wang[1]

Departments of [1]Sports Medicine, [2]Pathology, [4]Spine Surgery, Hainan General Hospital (Hainan Affiliated Hospital of Hainan Medical University), Haikou 570311, Hainan Province, China; [3]Department of Orthopaedic Surgery, Wuhan University People's Hospital, Wuhan 430000, Hubei Province, China. [*]Co-first authors.

Received April 30, 2021; Accepted August 26, 2021; Epub November 15, 2021; Published November 30, 2021

Abstract: Objective: To explore the molecular mechanisms underlying meniscus degeneration. Methods: We performed anterior cruciate ligament resection in the Hainan Wuzhishan pig to establish a meniscus degeneration model. We applied gene chip technology to detect differentially expressed genes (DEG) in the degenerative meniscus tissues. We applied Gene Ontology (GO), Kyoto Encyclopedia of Genes and Genomes (KEGG) pathway, core gene network, and relevant MicroRNA analyses to identify regulatory networks relevant to meniscus degeneration. We detected 893 differentially expressed genes, mainly involved in hormone production, apoptosis, and inflammation. Results: We found that *MUC13*, inflammatory mediator regulation of TRP channels, *MDFI*, and *miR-335-5p* may play a key role in the degenerative meniscus tissue. Conclusion: We found that meniscus degeneration involves several molecular mechanisms and provide molecular targets for future research into the disease.

Keywords: Differentially expressed genes, gene ontology, Kyoto encyclopedia of genes and genomes, MicroRNA, Wuzhishan pig, molecular targets

Introduction

Meniscal degeneration plays an important role in knee pain triggered by various factors. With the increase of age, the meniscus will degenerate in micro and macro aspects, leading to pain and knee joint dysfunction [1-3]. Meniscus degeneration can lead to osteoarthritis (OA) [4]. Protecting the meniscus and delaying the degeneration of the meniscus are critical to prevent meniscus injury in young and middle-aged patients, and relieves the symptoms of elderly patients with knee arthritis. The molecular mechanism underlying the meniscus degeneration remains largely unclear.

Yubo Sun et al. [5] reported that many genes involved in meniscus degeneration by participating in the biological processes of immune response, inflammatory response, biomineral formation, and cell proliferation. These were expressed at significantly higher levels in OA meniscal cells than in normal meniscal cells. Jun Zhao et al. [6] identified lncRNA and mRNA biomarkers in the degenerative meniscus of patients with OA. The results revealed 208 differentially expressed RNAs, including 32 lncRNAs and 176 mRNAs. These were primarily involved in collagen fibril organization, extracellular matrix organization, endothelial cell migration, *Staphylococcus aureus* infection, complement and coagulation cascades, and rheumatoid arthritis. Trauma, chronic inflammation and apoptosis may involve unilaterally or multilaterally in the process of meniscus degeneration. Countless genes may play a role in meniscus degeneration [7, 8], which makes the research on the mechanism of meniscus degeneration challenging.

The Gene-Cloud of Biotechnology Information (GCBI) laboratory performs gene chip data analysis online: (https://www.gcbi.com.cn/gclab/html/getLab/10025, 2021-1-20) [9]. In GCBI, complex biological information analysis can be completed just by dragging the 'move' module and clicking 'operation' [10]. Many studies [11-15] have used GCBI to discover new genes and

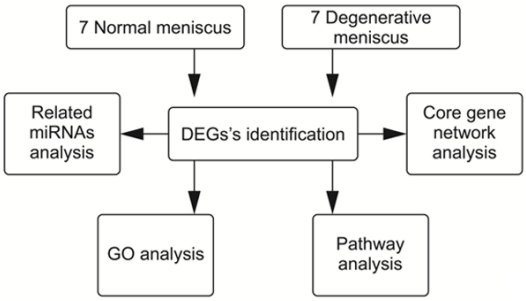

Figure 1. Flow diagram of the study design.

molecular mechanisms in diseases and to understand the underlying molecular mechanisms. Studies on meniscus degeneration by GCBI are scarce. In order to identify more candidate genes involved in meniscal degeneration by GCBI, we compared the expression profiles of degenerative meniscus with those of normal controls.

Materials and methods

Animals

A total of 14 healthy, adult male Hainan Wuzhishan pigs (Institute of Animal Husbandry and Veterinary Medicine, Hainan Academy of Agricultural Sciences, China) were randomly divided into a normal meniscus group and a meniscus degeneration group. Anterior cruciate ligament resection was performed in the meniscus degeneration group. The skin was cut in the normal meniscus group. The weight of the pigs was 15-18 kg, and the age was 6-7 months. Normal light/dark circulation, diet, and group feeding were provided. The environmental temperature was maintained at 20-28°C. All pigs were sacrificed 24 weeks after the operation. All operations were performed under pentobarbital sodium anaesthesia (20 mg/kg BW, Merck Serono KGaA, Darmstadt, Germany). The Ethics Committee of Hainan Provincial People's Hospital of China approved the experiment (Approval No: Med-Eth-Re [2018] 01). All methods were performed in accordance with the relevant guidelines and regulations of the Ethics Committee.

RNA extraction

The total RNA was extracted from meniscus tissues using E.Z.N. (Omega Bio-Tek Inc., Norcross, GA, USA) after DNase digestion, according to the manufacturer's instructions. The quantity and quality of the RNA were measured using a NanoDrop ND-1000 spectrophotometer (Thermo Fisher Scientific, Massachusetts, USA). RNA integrity was assessed by standard denatured agarose gel electrophoresis.

Microarray

The Pig Gene Expression 4x44K Microarray V2 (Agilent Technologies, Santa Clara, CA, USA) was used to compare mRNA expression profiles in normal and degenerative meniscus tissue. Microarray analysis was performed using the GCBI analysis platform [9].

Morphological observation and HE staining

The medial meniscus was taken out to observe the smoothness, gloss, and color of the surface. After cleaning, it was fixed with 10% formalin. After 72 hours, it was decalcified, dehydrated, embedded in paraffin, and then sectioned. After HE staining, the morphological and structural changes of the meniscus were observed under a microscope.

Strategy

The flow chart of the analysis is shown in **Figure 1**. Raw counts were used for testing differentially expressed genes (DEG) using the two-sample Welch's t-test (unequal variances). DEG was defined as genes with at least two-fold up- or down-regulation and an FDR controlled at 5%. DEG analysis adopted a literature method (SAM, Significance Analysis of Microarrays) to screen genes with significant differences under pre-set groups [16]. The two-sample Welch's *t*-test (unequal variances) was performed to identify mRNAs that showed significant ($P<0.05$) fold change (i.e., >1.5) between groups and presented a false discovery rate (FDR) <0.05. The identified DEGs were then sorted by *P*-value. The Gene Ontology (GO) system was used to classify the DEGs according to their biological functions. GO system is a database established by the Gene Ontology Consortium. It is a cross-species, comprehensive, and descriptive database. GO analysis annotates the gene function of the different genes between the two groups based on GO system to get all the functions involved by the genes. Fisher's exact test and multiple comparison test were used to calculate the

Table 1. Primer sequences for GAPDH, CYP2C33, GCNT7, and NCDN

GAPDH	F: 5' TCTCTGCTCCTCCCCGTT 3'
	R: 5' CGGCCAAATCCGTTCACT 3'
CYP2C33	F: 5' CATACATCGCCTTACTTCCTTCTAAC 3'
	R: 5' CTGAAGACAGTAGCGGCAATACA 3'
GCNT7	F: 5' GGCTTACACTGGCTTTAGGAG 3'
	R: 5' AGTTTGGCTTGTCTTGGATTTA 3'
NCDN	F: 5' AGACCTGCTGTCACATCTTCCTC 3'
	R: 5' AGCGACGCCATCAGAGTGTT 3'

significance level (*P*-value) of each function, to screen out the significant functions embodied by the difference genes. P<0.05 was set to distinguish statistically significant enrichment results. Kyoto Encyclopedia of genes and genomes (KEGG) pathway analysis was performed to identify the affected pathways. KEGG is a database for systematic analysis of the relationship between genes (and their coding products), gene function, and genome information. It helps researchers to study genes and expression information as a whole network. Based on KEGG database, Fisher's exact test was used to analyze the significance of the pathways involved in the target genes, to screen out the significant pathways embodied by the differential genes. P<0.05 was set as the significant pathway. DEGs were analysed by core gene network analysis and related miRNA analysis. The core gene network analysis displays the interaction between the input genes, which makes it easier for researchers to understand the core function of the input genes. The core network was based on the relationship between these genes and genes that have a database and literature basis in PubMed, Mesh, and KEGG databases. Related miRNA analysis showed at least two miRNAs that interact with the input gene. Related miRNAs were based on the relationship between genes and miRNAs that were documented in the PubMed and miRbase, to construct a network of related miRNAs. All data mentioned above were analysed by the GCBI analysis platform.

Real-time RT-PCR

Seven genes were selected for validation. The transcriptional level of the selected housekeeping gene, *GAPDH,* was quantified by the ViiA 7 Real-time PCR System (Applied Biosystems, Foster City, CA, USA). Primers were designed using Primer 5.0 (Premier Biosoft International, Palo Alto, CA, USA), and were based on the cDNA sequences in the NCBI sequence database (https://www.ncbi.nlm.nih.gov/refseq/, 2021-02-10). The main parameters are shown in **Table 1**. The Gene Amp PCR System 9700 (Applied Biosystems, Foster City, CA, USA) was used to generate the first chain cDNA from the separated RNA. According to the manufacturer's instructions, cDNA was amplified by performing the initial step of Taq DNA polymerase activation at 95°C for 10 minutes, followed by 40 denaturation cycles at 95°C for 10 seconds, and annealed at 60°C for 60 seconds. Each reaction was repeated three times. The Ct value of each gene was obtained in triplicate. The 2-ΔΔCt method [16] was used to normalize the expression level of the selected gene to that of *GAPDH*. Each real-time RT-PCR experiment was repeated in triplicate. The data of PT-PCR was analysed using SPSS 19.0 software (IBM, Armonk, NY, USA). Student's *t*-tests were used for comparisons between the two groups, and P<0.05 indicated statistical difference.

Results

Degeneration model in the Hainan Wuzhishan pig

A Wuzhishan pig in Hainan province of China is the smallest, lightest, and most endangered Chinese miniature pig. Its anatomy, physiological characteristics, and disease mechanism are very similar to humans. In our study, Wuzhishan pigs provided the additional advantages of body size, facilitated surgical procedures, and generated sufficient joint tissue for molecular analysis. In the normal meniscus group, the meniscus was smooth and complete, with a white and shiny surface, without any signs of degeneration. In the degenerative meniscus group, the surface of the meniscus was rough, the color was dim, the elasticity was poor, and there were some small defects and erosion (**Figure 2**). In the normal meniscus group, HE staining of the meniscus showed normal meniscus structure. In the degenerative meniscus group, HE staining of the meniscus showed disorder, uneven staining and sparse arrangement of collagen fibers, reduction and swelling of chondrocytes, reduction or disappearance of cartilage lacunae, increased local

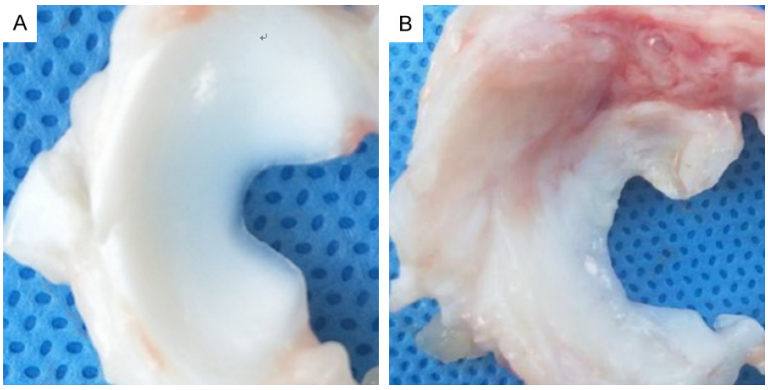

Figure 2. Meniscus in normal group and degeneration group. A: In the normal meniscus group, the meniscus was crescent shaped, with complete and smooth surface, no tear, white color and good elasticity. The medial part of the meniscus was thin, and the lateral part was thick. B: In the degenerative meniscus group, the color of the meniscus was light yellow, the elasticity was worse than that of the normal meniscus, the surrounding synovial membrane was congested with edema, the inner part was thinner with uneven wear, and the free edge was incomplete and cracked.

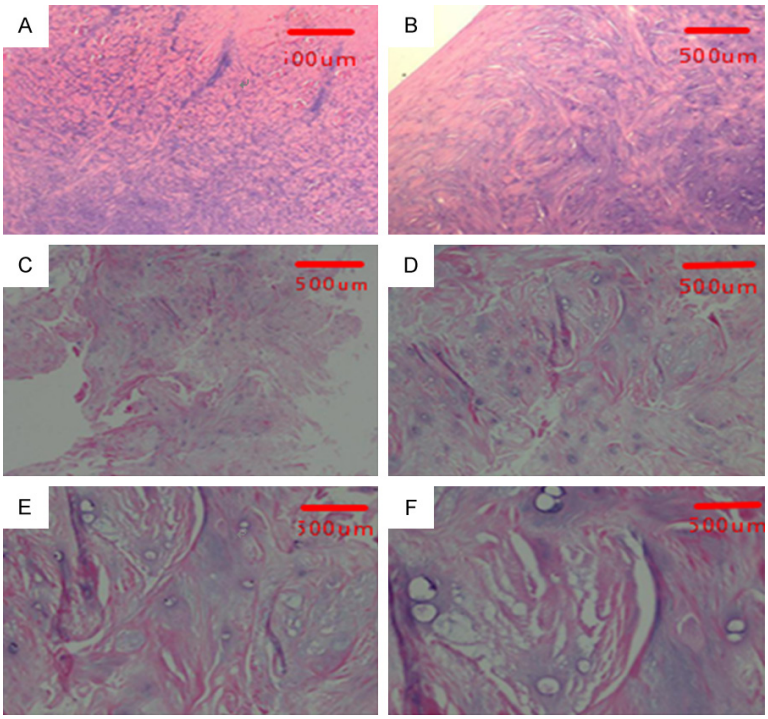

Figure 3. H-E staining of meniscus of normal group and degeneration group. A, B: The HE staining of normal meniscus tissue. The chondrocyte nucleus was large and round, the cell distribution was regular, the collagen fibers were abundant, and the fiber bundles were thick and neat. C-F: The HE staining of degenerative meniscus. The arrangement of collagen fibers was disordered, the staining was uneven, and the arrangement was sparse; the chondrocytes were arranged disorderly and reduced, and the visible cells were swollen, the cartilage lacuna was reduced or disappeared, and the local area was fibrotic and hyalinized. A: ×40, B: ×100, C: ×40, D: ×100, E: ×200, F: ×400.

fibers and hyaline changes, which were consistent with meniscal degeneration (**Figure 3**).

893 DEGs of degenerative meniscus tissue

There were 893 DEGs in the two groups, including 537 upregulated genes and 356 downregulated genes. The results are shown in the volcano plot and the dendrogram (**Figure 4**). The top 10 most significant genes were *CYP2C33, GCNT7, NCDN, EXD3, MUC13, PPP1R3D, NPHP3, UPB81, CD81*, and *PRPH* (**Table 2**).

GO analysis of 55 biological processes

A total of 55 biological processes enriched by the DEGs were obtained. The top 10 biological processes were cell response to hormone stimulus, response to hormones, sex determination, muscle fibre development, mesenchyme morphogenesis, cell response to endogenous stimulus, C21 steroid hormone metallic process, neuropeptide signalling pathway, negative regulation of the reactive oxygen species metallic process, and regulation of the nitric oxide biosynthetic process (**Table 3**).

Modulation of 36 pathway

A total of 36 pathways were modulated by the alteration of the gene expression. The top 10 pathways are Type II diabetes mellitus, thyroid hormone synthesis, taste transduction, prolactin signalling pathway, longevity regulating pathway, ovarian steroidogenesis, neuroactive ligand-receptor interaction, inflammatory

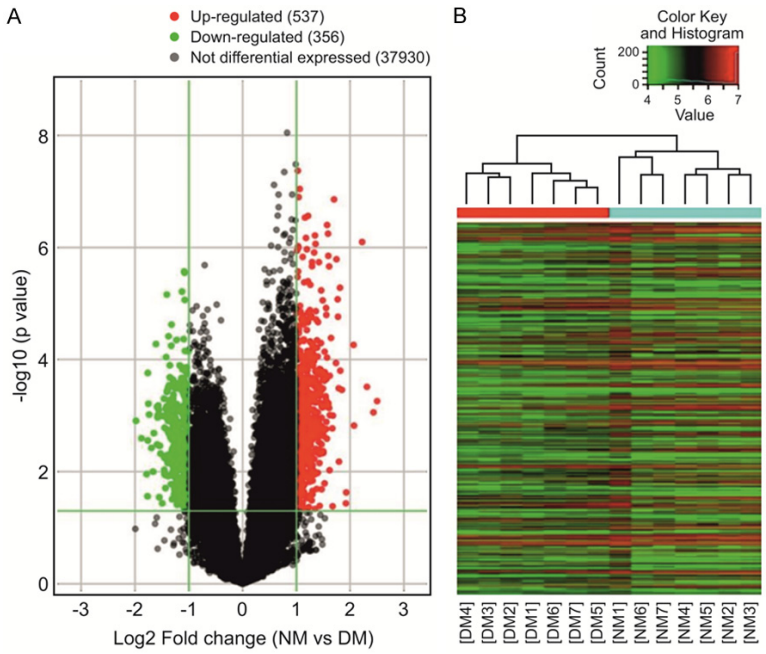

Figure 4. Volcano plot and heatmap of DEGs. A: Volcano plot. Red and green represent differentially expressed genes (DEGs); the downregulated DEGs are shown in green, and the upregulated DEGs are shown in red. B: The dendrogram. The ordinate represents the grouping information of the sample. Red indicates high relative expression and green indicates low relative expression. NM: normal meniscus; DM: degenerative meniscus.

mediator regulation of TRP channels, pantothenate and CoA biosynthesis, and cocaine addiction (**Table 4**).

Core gene network and 101 relevant miRNA analysis

Core network analysis yielded 40 core genes. *MDFI* had the largest number of connections, indicating that it was in the most core gene (**Figure 5**). The corresponding genes and data sources of *MDFI* are detailed in **Table 5**. Relevant miRNA analysis yielded 101 related miRNAs; of these, miR-335-5p was the most connected related miRNA (**Figure 6**). The correspondence and data source of miR-335-5p are detailed in **Table 6**.

Strong agreement between the microarray and RT-PCR results

To verify the reliability of the microarray results, the expression levels of the 10 genes (*CYP2C33, GCNT7, NCDN, EXD3, MUC13, PPP1R3D, NPHP3, UPB81, CD81*, and *PRPH*) were detected by RT-PCR and the results were consistent with the microarray data. The 10 genes were chosen because they showed maximum significance in the microarray results. The differential mRNA expression of *GCNT7, NCDN, EXD3, MUC13, PPP1R3D, NPHP3*, and *CD81* between the degenerative meniscus group and the normal meniscus group was statistically significant ($P<0.05$) (**Figure 7**). The results proved the strong agreement between the microarray and RT-PCR results.

Discussion

In this study, an Agilent-026440 *Sus scrofa* (Pig) Oligo Microarray v2 chip was used to detect DEGs in the degenerative meniscus tissue. There were 893 DEGs between the meniscus degeneration group and the normal group, of which 537 genes were upregulated, and 356 genes were downregulated. We found 10 genes with the most significant expression. They were *CYP2C33*, *GCNT7*, *NCDN*, *EXD3*, *MUC13*, *PPP1R3D*, *NPHP3*, *UPB1*, *CD81,* and *PRPH*. The transmembrane mucin encoded by *MUC13* has a variety of physiological functions, mainly to lubricate and protect the mucosal epithelium. Under pathological conditions, *MUC13* expression is abnormal and participates in the occurrence and development of inflammation and tumours [18, 19]. Our study found that *MUC13* was overexpressed in degenerative meniscus tissues, suggesting that it may play an important role in this process, presumably by exerting anti-inflammatory effects. IL-8 is an important inflammatory factor. MUC13 promotes NF-κB activity through NF-κB-dependent pathways and increases IL-8 production. OA synovial fluid contains high levels of IL-6 and IL-8 [20]. The increased expression of IL-8 has a chemotactic effect on inflammatory cells and stimulates the secretion of IL-6, promoting joint inflammation [20]. MUC13 may play a role in degenerative meniscus tissue through its anti-inflammatory effect.

Table 2. Top 10 most significant genes based on the comparative expression profiles of the degenerative and control menisci in a pig degeneration model

Probe Name	*P*-value	FDR	Fold Change	Regulation	Gene Symbol	Rank
A_72_P526917	1.2593E-07	0.000537464	2.0593695	up	*CYP2C33*	1
A_72_P362758	1.38326E-07	0.000537464	3.2506906	up	*GCNT7*	2
A_72_P050406	6.10533E-07	0.001031403	2.5418055	up	*NCDN*	3
A_72_P258107	8.6355E-07	0.001198329	2.5599119	up	*EXD3*	4
A_72_P165116	9.46523E-07	0.001225904	2.046065	up	*MUC13*	5
A_72_P442485	1.08108E-06	0.001272895	2.2891991	up	*PPP1R3D*	6
A_72_P222892	1.13988E-06	0.001302652	2.0178437	up	*NPHP3*	7
A_72_P234107	1.23101E-06	0.001328635	2.5152315	up	*UPB1*	8
A_72_P496803	1.4119E-06	0.001443671	3.0181273	up	*CD81*	9
A_72_P352838	1.81842E-06	0.001613149	2.4487246	up	*PRPH*	10

FDR: false discovery rate.

Table 3. The top 10 enriched GO terms for the DEGs by *P*-value in ascending order

Term	Count	*P*-value	Regulation	Rank
cellular response to hormone stimulus	7	0.000311929	Up	1
response to hormone	7	0.001152029	Up	2
sex determination	2	0.001281445	Down	3
muscle fibre development	2	0.002753211	Down	4
mesenchyme morphogenesis	2	0.002753211	Down	5
cellular response to endogenous stimulus	8	0.003566943	Up	6
C21-steroid hormone metabolic process	2	0.003588081	Up	7
neuropeptide signalling pathway	3	0.003940886	Up	8
negative regulation of reactive oxygen species metabolic process	2	0.004359628	Up	9
regulation of nitric oxide biosynthetic process	2	0.007086781	Up	10

Table 4. Enriched pathways for the differentially expressed genes (DEGs) identified by their comparative expression profiles in the degenerative and control menisci in a pig degeneration model

Definition	Fisher *P*-value	Regulation	Rank
Type II diabetes mellitus	0.000759595	Up	1
Thyroid hormone synthesis	0.002669959	Down	2
Taste transduction	0.002858715	Up	3
Prolactin signalling pathway	0.003352503	Up	4
Longevity regulating pathway	0.007875137	Up	5
Ovarian steroidogenesis	0.009215694	Up	6
Neuroactive ligand-receptor interaction	0.01021098	Up	7
Inflammatory mediator regulation of TRP channels	0.01098087	Up	8
Pantothenate and CoA biosynthesis	0.01205545	Up	9
Cocaine addiction	0.01468413	Down	10

According to the GO analysis, 55 biological processes were significantly expressed. After comprehensive analysis, the top 10 biological processes were cell response to hormone stimulus, response to hormones, sex determination, muscle fibre development, mesenchyme morphogenesis, cell response to endogenous stimulus, C21 steroid hormone metallic process, neuropeptide signalling pathway, negative regulation of reactive oxygen species, metallic process, and regulation of nitric oxide biosynthetic process. Studies [21-23] have reported that the inhibitory effect of sex hormones seems to be related to cystic degenera-

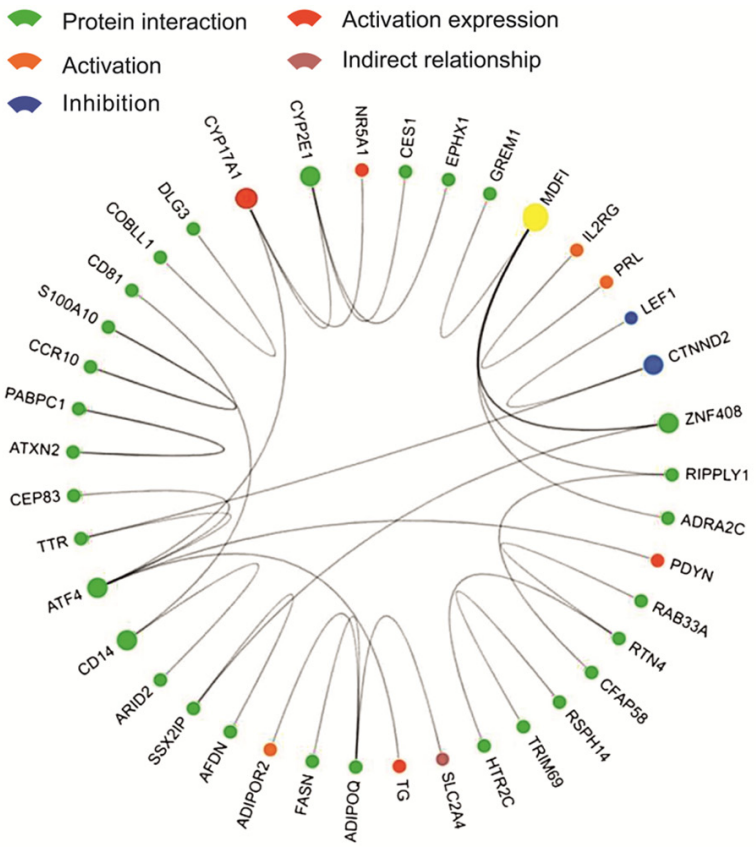

Figure 5. Interaction between core genes. Dots indicate core genes; lines between dots indicate relationships, and the colors of dots indicate specific relationships (see the icon in the upper left corner); larger dots indicate more relationships; yellow dots indicate genes with the most relationships (*MDFI*).

tion of meniscus tissue. Growth hormones and parathyroid hormones have effects on the meniscus and chondrocytes. NO is the main cause of human articular chondrocyte apoptosis [24-27]. These studies are consistent with our findings. The regulatory biosynthesis of nitric oxide is one of the most enriched biological processes in GO analysis. Studies have shown that NO induces chondrocyte apoptosis. NO is the main cause of human articular chondrocyte apoptosis [24, 28-31]. Our study shows that No is involved in the biological process of meniscus degeneration, indicating that NO induced apoptosis of meniscus cells also occurs, which could eventually lead to the degeneration of meniscus tissue. The consistency between our findings and previous studies strongly supports our hypothesis that degenerated meniscus cells are different from normal meniscus cells.

Inflammatory mediator regulation of TRP channels was one of the 10 lowest *P*-values in the pathway analysis. With a variety of cellular signal receptors, it plays a very important role in the inflammatory response [32, 33]. In this study, we found that the inflammatory mediators of TRP channel were up-regulated in the degenerative meniscus, indicating that the degeneration of meniscus is related to TRP channel and inflammatory response.

MDFI and miR-335-5p identified in this study, both regulate the WNT signalling pathway [34, 35], which is a core signal pathway of OA synovitis [36, 37]. The result showed that synovitis and meniscal degeneration may have similar mechanisms of action. Synovial and meniscal tissues are also involved in the pathogenesis of OA. Tornero-Esteban's [38] study showed a correlation between miR-335-5p expression and OA. The possible mechanism is that miRNA-335-5p alleviates inflammation in OA chondrocytes through activation of autophagy [39]. Our study found a strong correlation between miR-335-5p and meniscus degeneration. MiR-335-5p may play an important role in meniscus degeneration, indicating that miR-335-5p may become a new target for clinical prevention and treatment of meniscus degeneration. The specific mechanism of mediating meniscus degeneration will be the focus of follow-up research.

There are some shortcomings in this study. The 'knee' joint in pigs is different from humans in biomechanics. The animal model research cannot be completely equivalent to the study of meniscus degeneration in human patients. This model is similar to traumatic meniscus degeneration, such as human meniscus and cruciate ligament injury, rather than primary meniscus degeneration. Considering the various challenges (such as the ethical issues) involved with the study of human specimens, the difficulty of obtaining a sufficient sample

Table 5. The Correspondence and data source of *MDFI*

Gene 1	Protein 1	Gene 2	Protein 2	Relationship	Experiment	Source
MDFI	Q99750	GREM1	O60565	protein interaction	two hybrid array	PMID: unassigned 1304
MDFI	Q99750	ZNF408	Q9H9D4	protein interaction	two hybrid array	PMID: 19060904
MDFI	Q99750	ZNF408	Q9H9D4	protein interaction	two hybrid array	PMID: unassigned 1304
MDFI	Q99750	ZNF408	Q9H9D4	protein interaction	two hybrid pooling approach	PMID: 16189514
MDFI	Q99750	RIPPLY1	Q0D2K3	protein interaction	two hybrid array	PMID: unassigned 1304
MDFI	Q99750	ADRA2C	P18825	protein interaction	two hybrid array	PMID: unassigned 1304

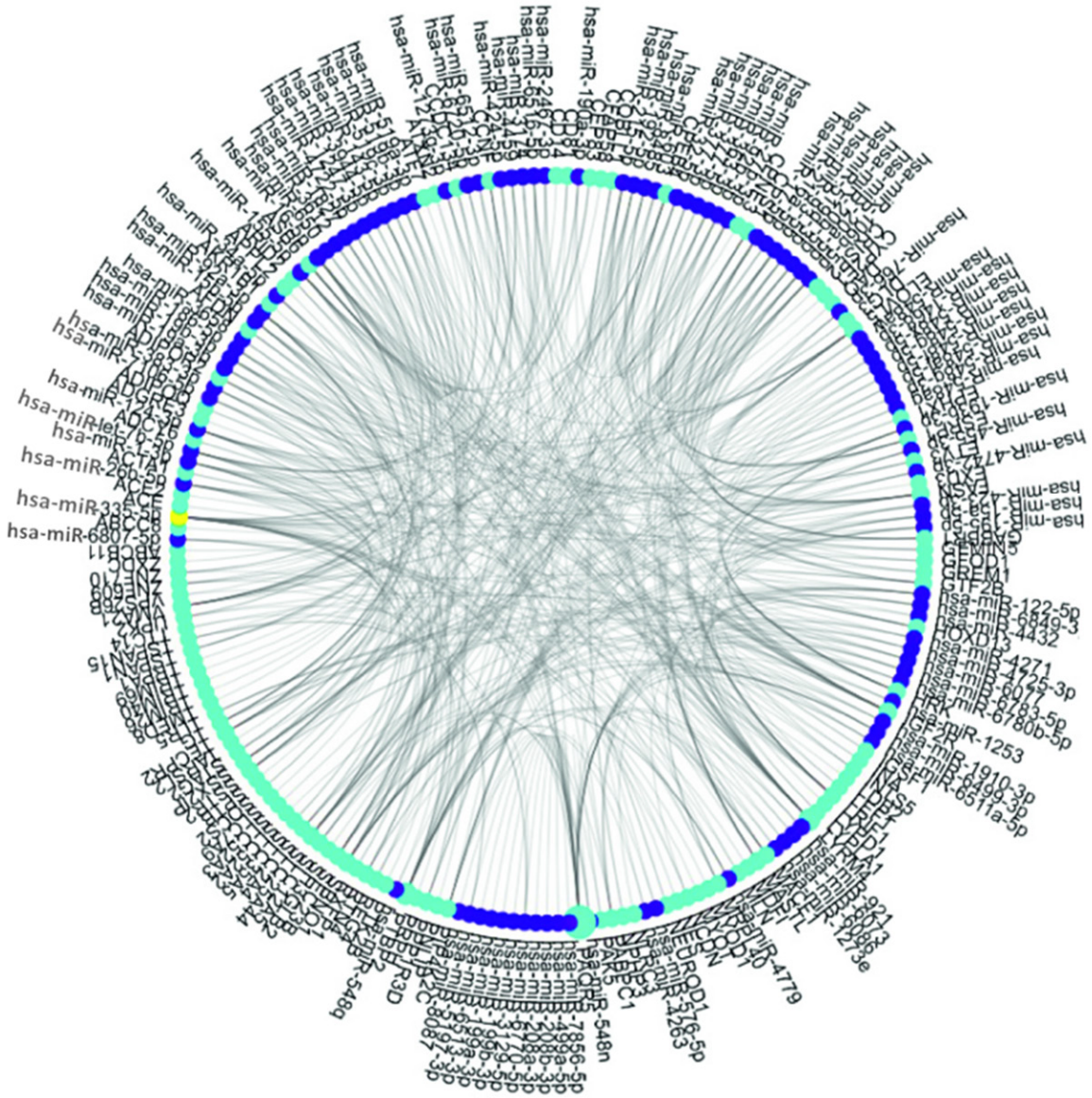

Figure 6. The relationship network between DEGs and miRNAs. Royal blue dots indicate DEGs; purple dots indicate miRNAs; larger dots indicate more relationships; yellow dots indicate miRNAs with the most relationships (miR-335-5p). DEGs, differentially expressed genes. miRNAs, microRNA.

size, the obvious heterogeneity of specimens, and the difficulty of obtaining specimens from special body parts, this animal model is an ideal research tool.

Table 6. The Correspondence and data source of miR-335-5p

MiRNA name	Target gene name	Experimental verification method	PMID
miR-335-5p	ABCC8	Microarray	18185580
miR-335-5p	ACE	Microarray	18185580
miR-335-5p	ADCY6	Microarray	18185580
miR-335-5p	ADGRE3	Microarray	18185580
miR-335-5p	AFDN	Microarray	18185580
miR-335-5p	CD14	Microarray	18185580
miR-335-5p	CFAP58	Microarray	18185580
miR-335-5p	CPEB4	Microarray	18185580
miR-335-5p	CYP2E1	Microarray	18185580
miR-335-5p	DLG3	Microarray	18185580
miR-335-5p	ESRP1	Microarray	18185580
miR-335-5p	EXD3	Microarray	18185580
miR-335-5p	GABBR1	Microarray	18185580
miR-335-5p	MACF1	Microarray	18185580
miR-335-5p	MDFI	Microarray	18185580
miR-335-5p	MLN	Microarray	18185580
miR-335-5p	MYOD1	Microarray	18185580
miR-335-5p	MYOT	Microarray	18185580
miR-335-5p	NCDN	HITS-CLIP	27418678
miR-335-5p	PNLIP	Microarray	18185580
miR-335-5p	PPP1R3D	Microarray	18185580
miR-335-5p	PTK2B	Microarray	18185580
miR-335-5p	SLC2A4	Microarray	18185580
miR-335-5p	SLC35A5	HITS-CLIP	23313552
miR-335-5p	SLC7A9	Microarray	18185580
miR-335-5p	SPTB	Microarray	18185580
miR-335-5p	TRIM40	Microarray	18185580
miR-335-5p	TRIM69	Microarray	18185580
miR-335-5p	TSPAN15	Microarray	18185580
miR-335-5p	ZNF609	Microarray	18185580

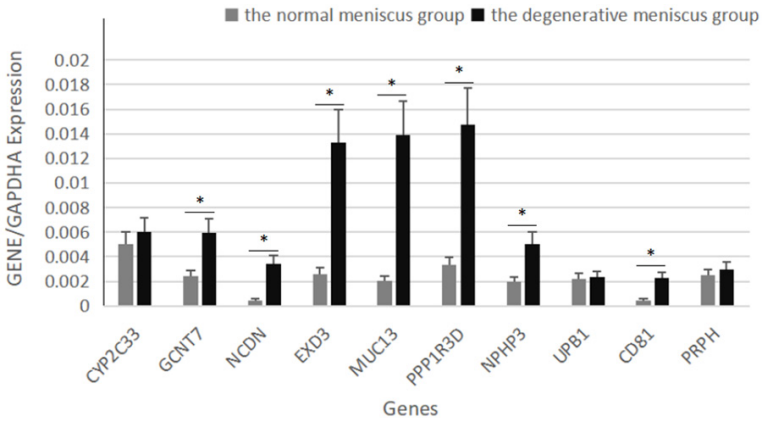

Figure 7. Verification of 10 selected genes by real-time RT-PCR for their comparative expression profiles in the degenerative and control menisci in a pig degeneration model. Error bars indicate the mean ± standard errors of the mean (*P<0.05).

In summary, our study presents a comprehensive bioinformatics analysis of meniscus degeneration. The results may help us to improve our understanding of the molecular mechanisms underlying meniscus degeneration. MDFI and miR-335-5p may represent targets for the diagnosis and treatment of meniscus degeneration.

Acknowledgements

This work was supported by Key R&D plan of Hainan Province, China (grant number ZDYF2019180), and Scientific Research Project of the Health Industry in Hainan Province, China (grant number 20A200488).

Disclosure of conflict of interest

None.

Address correspondence to: Drs. Guangji Wang and Daolu Zhan, Hainan General Hospital (Hainan Affiliated Hospital of Hainan Medical University), 31 Longhua Road, Longhua District, Haikou 570311, Hainan Province, China. Tel: +86-0898-68613-527; E-mail: guangjiwang@yeah.net (GJW); 85796852@qq.com (DLZ)

References

[1] Howell R, Kumar NS, Patel N and Tom J. Degenerative meniscus: pathogenesis, diagnosis, and treatment options. World J Orthop 2014; 5: 597-602.

[2] Yuan X, Arkonac DE, Chao PG and Vunjak-Novakovic G. Electrical stimulation enhances cell migration and integrative repair in the meniscus. Sci Rep 2014; 4: 3674.

[3] Goetz JE, Coleman MC, Fredericks DC, Petersen E,

Martin JA, McKinley TO and Tochigi Y. Time-dependent loss of mitochondrial function precedes progressive histologic cartilage degeneration in a rabbit meniscal destabilization model. J Orthop Res 2017; 35: 590-599.
[4] López-Franco M, López-Franco O, Murciano-Antón MA, Cañamero-Vaquero M, Fernández-Aceñero MJ, Herrero-Beaumont G and Gómez-Barrena E. Meniscal degeneration in human knee osteoarthritis: in situ hybridization and immunohistochemistry study. Arch Orthop Trauma Surg 2016; 136: 175-183.
[5] Sun Y, Mauerhan DR, Honeycutt PR, Kneisl JS, Norton JH, Hanley EN Jr and Gruber HE. Analysis of meniscal degeneration and meniscal gene expression. BMC Musculoskelet Disord 2010; 11: 19.
[6] Sun Y and Mauerhan DR. Meniscal calcification, pathogenesis and implications. Curr Opin Rheumatol 2012; 24: 152-157.
[7] Aigner T, Fundelm K, Saas J, Gebhard PM, Haag J, Weiss T, Zien A, Obermayr F, Zimmer R and Bartnik E. Large-scale gene expression profiling reveals major pathogenetic pathways of cartilage degeneration in osteoarthritis. Arthritis Rheum 2006; 54: 3533-44.
[8] Brophy RH, Sandell LJ, Cheverud JM and Rai MF. Gene expression in human meniscal tears has limited association with early degenerative changes in knee articular cartilage. Connect Tissue Res 2016; 58: 295-304.
[9] The Gene-Cloud of Biotechnology Information (GCBI). https://www.gcbi.com.cn/gclab/html/getLab/10025, 2021-1-20.
[10] Huang H, Zheng J, Shen N, Wang G, Zhou G, Fang Y, Lin J and Zhao J. Identification of pathways and genes associated with synovitis in osteoarthritis using analyses. Sci Rep 2018; 8: 10050.
[11] Feng A, Tu Z and Yin B. The effect of HMGB1 on the clinicopathological and prognostic features of non-small cell lung cancer. Oncotarget 2016; 7: 20507-20519.
[12] Lu Y, Qin B, Hu H, Zhang J, Wang Y, Wang Q and Wang S. Integrative microRNA-gene expression network analysis in genetic hypercalciuric stone-forming rat kidney. PeerJ 2016; 4: e1884.
[13] Yang Z, Xu S, Jin P, Yang X, Li X, Wan D, Zhang T, Long S, Wei X, Chen G, Meng L, Liu D, Fang Y, Chen P, Ma D and Gao Q. MARCKS contributes to stromal cancer-associated fibroblast activation and facilitates ovarian cancer metastasis. Oncotarget 2016; 7: 37649-37663.
[14] Gao JR, Qin XJ, Jiang H, Wang T, Song JM and Xu SZ. Screening and functional analysis of differentially expressed genes in chronic glomerulonephritis by whole genome microarray. Gene 2016; 589: 72-80.
[15] Ling Q, Xie H, Li J, Liu J, Cao J, Yang F, Wang C, Hu Q, Xu X and Zheng S. Donor graft MicroRNAs: a newly identified player in the development of new-onset diabetes after liver transplantation. Am J Transplant 2017; 17: 255-264.
[16] Takagaki N, Ohta A, Ohnishi K, Kawanabe A, Minakuchi Y, Toyoda A, Fujiwara Y and Kuhara A. Identification of differentially expressed gene transcripts in porcine endometrium during early stages of pregnancy. EMBO Rep 2020; 21: e48671.
[17] Reis M, Vieira P, Morales C and Ramiro H. Fold change in regucalcin expression after chill-coma recovery (ChCR) obtained by qRT-PCR using the 2-ΔΔCt method. PLoS One 2011; 6: e25520.
[18] Gupta B, Sikander M and Jaggi M. Overview of mucin (MUC13) in gastrointestinal cancers. J Gastroenterol Dis 2016; 1: 18-19.
[19] Sheng YH, Triyana S, Wang R, Das I, Gerloff K, Florin TH, Sutton P and McGuckin MA. MUC1 and MUC13 differentially regulate epithelial inflammation in response to inflammatory and infectious stimuli. Mucosal Immunol 2013; 6: 557-568.
[20] Zhang B, Ren J, Yan X, Huang X, Ji H, Peng Q, Zhang Z and Huang L. Investigation of the porcine MUC13 gene: isolation, expression, polymorphisms and strong association with susceptibility to enterotoxigenic Escherichia coli F4ab/ac. Anim Genet 2008; 39: 258-266.
[21] Rokkanen P, Paatsama S and Rissanen P. The influence of certain hormones on the meniscus of the femoro-tibial (stifle) joint: a histological and histo-quantitative study on young dogs. J Small Anim Pract 1967; 8: 221-227.
[22] Noone TJ, Millis DL, Korvick DL, Athanasiou K, Cook JL, Kuroki K and Buonomo F. Influence of canine recombinant somatotropin hormone on biomechanical and biochemical properties of the medial meniscus in stifles with altered stability. Am J Vet Res 2002; 63: 419-426.
[23] Huang H, Skelly JD, Ayers DC and Song J. Age-dependent changes in the articular cartilage and subchondral bone of C57BL/6 mice after surgical destabilization of medial meniscus. Sci Rep 2017; 7: 42294.
[24] Blanco FJ, Ochs RL, Schwarz H and Lotz M. Chondrocyte apoptosis induced by nitric oxide. Am J Pathol 1995; 146: 75-85.
[25] Shen P, Nguyen M, Fuchs M, Reisener MJ and Löhning M. TLR1/2 signaling impairs mitochondrial oxidative phosphorylation in human chondrocytes via the induction of nitric oxide. Osteoarthritis Cartilage 2020; 28: S119.
[26] Kobayashi K, Mishima H, Hashimoto S, Goomer RS and Amiel D. Chondrocyte apoptosis and regional differential expression of nitric oxide in the medial meniscus following partial meniscectomy. J Orthop Res 2010; 19: 802-808.
[27] Kao XB, Chen Q, Gao Y, Fan P, Chen JH, Wang ZL, Wang YQ, Chen YN and Yan YP. SP600125 blocks the proteolysis of cytoskeletal proteins

in apoptosis induced by gas signaling molecule (NO) via decreasing the activation of caspase-3 in rabbit chondrocytes. Eur J Pharmacol 2018; 824: 40-47.
[28] Kim S, Hwang S, Shin DY, Kang S and Chun J. p38 kinase regulates nitric oxide-induced apoptosis of articular chondrocytes by accumulating p53 via NFκB-dependent transcription and stabilization by serine 15 phosphorylation. J Biol Chem 2002; 277: 33501-33508.
[29] Relić B, Bentires-Alj M, Ribbens C, Franchimont N, Guerne PA, Benoît V, Merville MP, Bours V and Malaise MG. TNF-α protects human primary articular chondrocytes from nitric oxide-induced apoptosis via nuclear factor-κB. Lab Invest 2002; 82: 1661-1672.
[30] Surendran S, Kim SH, Jee BK, Ahn SH, Goinathan P and Han CW. Anti-apoptotic Bcl-2 gene transfection of human articular chondrocytes protects against nitric oxide-induced apoptosis. J Bone Joint Surg Br 2006; 88: 1660-1665.
[31] Zhou Y, Ming J, Li Y, Deng M, Chen Q, Ma Y, Chen Z, Zhang Y and Liu S. Ligustilide attenuates nitric oxide-induced apoptosis in rat chondrocytes and cartilage degradation via inhibiting JNK and p38 MAPK pathways. J Cell Mol Med 2019; 2: 3357-3368.
[32] Ramirez GA, Coletto LA, Sciorati C, Bozzolo EP, Manunta P, Rovere-Querini P and Manfredi AA. Ion channels and transporters in inflammation: special focus on TRP channels and TRPC6. Cells 2018; 7: 70.
[33] Oehler B, Kistner K, Martin C, Schiller J, Mayer R, Mohammadi M, Sauer RS, Filipovic MR, Nieto FR, Kloka J, Pflücke D, Hill K, Schaefer M, Malcangio M, Reeh PW, Brack A, Blum R and Rittner HL. Inflammatory pain control by blocking oxidized phospholipid-mediated TRP channel activation. Sci Rep 2017; 7: 5447.
[34] Zhang J, Tu Q, Bonewald LF, He X, Stein G, Lian J and Chen J. Effects of miR-335-5p in modulating osteogenic differentiation by specifically downregulating Wnt antagonist DKK1. J Bone Miner Res 2011; 26: 1953-1963.
[35] Wang Q, Young TM, Mathews MB and Pe'ery T. Developmental regulators containing the I-mfa domain interact with T cyclins and Tat and modulate transcription. J Mol Biol 2007; 367: 630-646.
[36] Van den Bosch MH, Blom AB, Sloetjes AW, Koenders MI, van de Loo FA, van den Berg WB, van Lent PL and ven der Kraan PM. Induction of canonical Wnt signaling by synovial overexpression of selected Wnts leads to protease activity and early osteoarthritis-like cartilage damage. Am J Pathol 2015; 185: 1970-1980.
[37] Kitanaka T, Nakano R, Kitanaka N, Kimura T, Okabayashi K, Narita T and Sugiya H. JNK activation is essential for activation of MEK/ERK signaling in IL-1β-induced COX-2 expression in synovial fibroblasts. Sci Rep 2017; 7: 39914.
[38] Tornero-Esteban P, Rodríguez-Rodríguez L, Abásolo L, Tomé M, López-Romero P, Herranz E, González MA, Marco F, Moro E, Fernández-Gutiérrez B and Lamas JR. Signature of microRNA expression during osteogenic differentiation of bone marrow MSCs reveals a putative role of miR-335-5p in osteoarthritis. BMC Musculoskelet Disord 2015; 16: 182.
[39] Zhong G, Long H, Ma S, Shunhan Y, Li J and Yao J. MiRNA-335-5p relieves chondrocyte inflammation by activating autophagy in osteoarthritis. Life Sci 2019; 226: 164-172.